A challenge for x-ray photoelectron spectroscopy characterization of Cu(In,Ga)Se2 absorbers: The accurate quantification of Ga/(Ga + In) ratio

Solène Béchu, Anais Loubat, Muriel Bouttemy, Jackie Vigneron, Jean-Louis Gentner, Arnaud Etcheberry

▶ **To cite this version:**

Solène Béchu, Anais Loubat, Muriel Bouttemy, Jackie Vigneron, Jean-Louis Gentner, et al.. A challenge for x-ray photoelectron spectroscopy characterization of Cu(In,Ga)Se2 absorbers: The accurate quantification of Ga/(Ga + In) ratio. Thin Solid Films, 2019, 669, pp.425-429. ⟨10.1016/j.tsf.2018.11.029⟩. ⟨hal-03116822⟩

HAL Id: hal-03116822

https://hal.science/hal-03116822v1

Submitted on 20 Jan 2021

HAL is a multi-disciplinary open access archive for the deposit and dissemination of scientific research documents, whether they are published or not. The documents may come from teaching and research institutions in France or abroad, or from public or private research centers.

L'archive ouverte pluridisciplinaire **HAL**, est destinée au dépôt et à la diffusion de documents scientifiques de niveau recherche, publiés ou non, émanant des établissements d'enseignement et de recherche français ou étrangers, des laboratoires publics ou privés.

HAL Authorization

A challenge for X-Ray Photoelectron Spectroscopy characterization of $Cu(In,Ga)Se_2$ absorbers: the accurate quantification of Ga / (Ga + In) ratio

Solène Béchu[1,2], Anais Loubat[1,2], Muriel Bouttemy[1,2], Jackie Vigneron[1,2], Jean-Louis Gentner[3], Arnaud Etcheberry[1,2]*

[1] Institut Photovoltaïque d'Ile-de-France (IPVF), 30 RD 128, 91120 Palaiseau, France.

[2] Institut Lavoisier de Versailles (ILV), Université Paris-Saclay, CNRS-UVSQ, 45 av. des Etats-Unis, Versailles, 78035, France.

[3] Almae Technologies SAS, Route de Nozay, 91460 Marcoussis, France

* *Corresponding author: arnaud.etcheberry@uvsq.fr*

Abstract

CIGS ($Cu(In,Ga)Se_2$) layers are among the more efficient photovoltaic absorbers for thin film solar cells and remain competitive in the worldwide landscape of solar cells devices and modules with also new emerging markets (flexible or metallic substrates, tandem, low or high band gap CIGS…). Their properties are governed by different key composition parameters, and among them the GGI ratio ([Ga]/[Ga]+[In])) which controls the gap value. Indeed, the GGI determination is an important metrological challenge at the surface of the CIGS layer, particularly before the buffer deposition. Using X-Ray Photoelectron Spectroscopy (XPS), we propose here a specific methodology to determine this ratio at the surface. In order to, a surface preparation of the CIGS by chemical treatments, combining an initial flattening by $HBr:Br_2:H_2O$ etching with a finishing step performed in $KCN:H_2O$, is implemented. This chemical engineering leads to a quasi "perfect" surface, flattened and cleared from surface oxide and selenide phase on which our XPS methodology for GGI determination is tested. The photopeaks choice to obtain the most coherent GGI ratio quantification is discussed. In

particular we focus on the Ga3d-In4d region, situated in narrow binding energy domain, and discuss why this photopeak combination can be considered as the most adapted for a representative GGI determination. Quantitative fitting procedure of the Ga3d-In4d region is qualified on a reference epitaxial $In_xGa_{1-x}As$ layer and its implementation in the CIGS case is shown.

Keywords

copper indium gallium selenide; X-ray photoelectron spectroscopy; Surface composition; Gallium; Indium; Surface chemical engineering

1. Introduction

X-ray Photoelectron Spectroscopy (XPS) on CIGS ($Cu(In,Ga)Se_2$) is an efficient method to provide surface chemical and quantitative information. The probed thickness is less than 10 nm when X-Ray excitation is provided by the Al-Kα line. It is inside this thin external layer region that most of the crucial chemical engineering processes are conducted for all the CIGS based devices. So, determination of the CIGS surface chemistry is still a challenge which needs specific and reliable approaches as it will enable to efficiently orientate the surface chemistry and, so, to optimize properties at the CIGS front and back interfaces. This paper aims to contribute providing XPS characterizations of CIGS absorbers, starting from reference CIGS surface to certify the quantitative composition approach, to further extended on real practical cases. The CIGS surfaces have their proper chemical specificities, emphasized by the complexity of the surface parameters as poly-crystallinity, roughness, local surface steps, side chemical perturbations, differential grain boundaries reactivity and grains crystallographic orientations. Considering all these combined complex factors in addition to the quaternary character of the alloy, it is obvious that chemical composition determination must still be considered as a challenge to be taken up.

Our paper deals with this issue and is focused on a methodological approach enabling to determine as precisely as possible the GGI ratio: ([Ga]/[Ga]+[In])) of CIGS absorber, main parameter, which governs the gap value [1-9]. Determining the exact GGI value is a central and difficult challenge for the cell conception. In particular, the surface absorber composition conditions the absorber/buffer layer interface energy diagram, then further cell efficiency issues. Considering the high surface sensitivity of XPS, this technique is a perfect nondestructive tool for the GGI determination of the outer part of the CIGS layer. To conduct a rigorous discussion, our metrological approach was first performed on reference CIGS surfaces presenting controlled surface chemistries. Reference surfaces can be obtained immediately after the layer growth, when it is possible, but also on a refreshed surface thanks to specific chemical treatments. In any case, for the present purpose, reference surfaces need to be oxides free, as well as free from binary selenide phases and all other side components, as sodium, commonly present on aged surfaces. Concerning CIGS, a “perfect-chemical” surface can be obtained by a combination of acidic [1], basic [10] and KCN aqueous treatments [10-14]. Possible combination [1] takes advantage of each treatment specificity to sequentially eliminate the surface oxides, the side binary selenide compounds and the elementary selenium. Nevertheless, the initial important roughness of CIGS surface is maintained. For a rigorous quantitative XPS approach, disposing of flattened surfaces up to few nanometers RMS (Root Mean Square) is also benefic to avoid relief artifacts (electrons backscattering…) and guarantee the homogeneity of the depth probed and the spatial origin of the photoelectrons.

In the present paper, a flattening step is then considered to help, at first, the fundamental quantitative approach by XPS analysis. It is obtained through a short time dipping in dilute aqueous acidic Br_2 solution [15]. This etching step is completed by a final chemical cleaning to reach the targeted CIGS “reference” surface, oxide or selenide side phases free at the XPS detection limit. The access to the actual GGI value and not to an estimation is not so evident because, if compositional XPS data are easy to obtain, their transformation in actual composition of alloys is more complex due to the quantification procedure involving inherently a necessary correction of the photopeak area

(transmission, sensitivity factors values, escape depth model…) and other uncontrolled side perturbations among them the carbon surface contamination is of particular importance. Indeed, carbon surface contamination has to be considered as an attenuation factor of the photopeaks intensities measured. This attenuation varies with kinetic energies (KE) of the different main core levels used and distributed along the whole KE scale. So, adventitious carbon operates as a differential filter for photoelectrons with different KE. This induces possible differences between the XPS estimation obtained by different photopeaks combination employed for quantification and the reality of the alloy composition of the treated surface. In this paper we discuss the use of the Ga3d-In4d region, in narrow binding energy region. It can be consider as the better alternative to provide the closer value to the actual surface GGI determination. The interest of considering this specific energy window gathering Ga3d and In4d, in addition to the conventional Ga2p and In3d peaks, has been previously introduced by Bär et al. [16,17]. In the present work, we extend the argumentation to use the Ga3d-In4d spectral window to have a direct overview of GGI evolution. This narrow binding energy region allows working with equivalent escape depth and carbon attenuation levels. So a more accurate GGI determination is expected. To comfort the Ga3d-In4d window exploitation, a fitting procedure is developed on a reference surface of $In_xGa_{1-x}As$ desoxidized epilayer. For this III-V alloy, the GGI ratio value is ensured by a fine determination via other complementary characterization method. We show that the metallurgic composition of this reference alloy can therefore also be well determined by XPS. We discuss the extension of the fitting procedure to the practical case of the reference CIGS surface.

2. Experiments

2.1. CIGS and InGaAs samples description and surfaces preparation by chemical engineering

The CIGS samples are supplied by ZSW (Zentrum für Sonnenenergie- und Wasserstoff-Forschung, Germany) [18].

CIGS is co-evaporated on Mo (600 nm) / glass (3 mm) substrates. The CIGS layers are provided with optimal GGI bulk ratio close to 0.30 and a thickness of 2.1 µm. A large area sample was divided in equivalent area pieces (1x1 cm) to ensure the reliability of the comparative diagnostic. In the present case, the absence of usual Ga gradient in depth was verified through Secondary Ion Mass Spectrometry (SIMS) measurements, performed on an IMS7f CAMECA. Those results are not presented here.

$In_xGa_{1-x}As$ epi-layer sample was grown by Metal Organic Vapors Phase Epitaxy process on InP (100). Sample thickness is nominally 160 nm which implies that the epitaxial layer is strained (no relaxation) on the InP substrate, then the Vegard Law can be used to determine by XRD (X-Ray Diffraction) the alloy composition. So the alloy composition of our reference layer has been derived from XRD rocking curve measurement and given as $In_{0.517}Ga_{0.483}As$.

The CIGS samples flattening is obtained thanks to an etching solution of HBr (0.20 mol L^{-1}): Br_2 (0.02 mol L^{-1}): H_2O (ultra-pure de-ionized water, 18.2 MΩ) [15]. This etching process allowing a quasi layer by layer dissolution of the CIGS absorber is not selective and leaves the surface deoxidized and leads to a spectacular decrease of the surface roughness. More details can be found elsewhere [15, 19]. As Ga gradient is not present on the used samples (as confirmed by SIMS profiling measurements), the XPS responses do not depend on the immersion time. The etching time is fixed to obtain a smooth surface, still conformal and thick at the XPS scale. Samples are rinsed under ultra-pure de-ionized water (18.2 MΩ) and dried with nitrogen flux. Then, as conventionally employed during the cell fabrication process, a wet chemical treatment based on a basic solution is performed using KCN (0.1 mol L^{-1}, 5 min) [10-14]. $In_xGa_{1-x}As$ sample is deoxidized using an HCl solution (2 mol L^{-1}, during 5 min). Finally, both CIGS and $In_xGa_{1-x}As$ samples are rinsed in ultra-pure water (18.2 MΩ), dried under nitrogen and directly transferred into the XPS spectrometer.

2.2. X-ray Photoelectron Spectroscopy (XPS)

XPS surface chemical analyses are carried out with a Thermo Electron K-Alpha$^+$ spectrometer using a monochromatic Al-Kα X-Ray source (1486.6 eV). The X-Ray spot size is 400 µm. The Thermo Electron procedure was used to calibrate the K-Alpha$^+$ spectrometer by using metallic Cu and Au samples intern references (Cu $2p_{3/2}$ at 932.6 eV and Au $4f_{7/2}$ at 84.0 eV). High energy resolution spectra are acquired using a Constant Analyser Energy mode 10 eV and 0.05 eV as energy step size. Data are processed using the Thermo Fisher scientific Avantage© data system. XPS spectra are treated using a Shirley background subtraction and XPS composition are deduced using the Sensitivity Factors, the transmission factor and inelastic mean-free paths from Avantage© library associated to the spectrometer. The fits are performed with Gaussian/Lorentzian mix.

3. Results and Discussion

As previously shown, aqueous acidic bromide solutions [15] generate a constant etching rate process which progressively eliminates the initial roughness of the layers. Our final RMS roughness is always in the 5-10 nm range, compared to the 100-150 nm initial ones. However if the spectacular flattening is easily reachable, a question is the associated post etching surface chemistry. Figure 1 shows the XPS evolutions of the as-grown, of the HBr:Br_2:H_2O and then of the HBr:Br_2:H_2O and KCN treated surfaces. Modifications are observed for the Ga3d-In4d and Se3d regions, as well as for the regular core levels used in the literature Ga$2p_{3/2}$, Cu$2p_{3/2}$ and In$3d_{5/2}$. Starting from an initial oxidized CIGS surface [1], Br_2 etching [15] leaves CIGS surfaces without oxide layer but with low side Se^0 phase which amount depends strongly on the etching conditions. When it is presented, the Se^0 side phase on Se3d peak is evidenced by an additional feature with a shoulder contribution in the 56-57 eV range. This feature disappears after KCN treatment (Figure 1-a). The deoxidation efficiency is evident on the O1s signal, whose intensity is drastically decreased, after HBr:Br_2:H_2O etching (Figure 1-d). Moreover the Ga and In photopeaks present strongly thinned envelops and the characteristic oxide contribution of the Se3d close to 59 eV disappears. All the photopeaks present higher intensities

after chemical treatments, in accordance with the decrease of the superficial carbon contamination (Figure 2). A qualitative comparison between those intensities evolution show an expected Cu-depletion on the as-grown [1]. Finally, the Cu signals $Cu2p_{3/2}$ and Cu(LMM) Auger lines (not shown here) of the chemically treated samples are characteristic of a Cu(I) contribution as expected for a CIGS lattice. Note that in this case, the possible Cu_2O contribution which is difficult to discriminate from Cu(I) in CIGS is easily eliminated due to the very low oxygen level and comforted because an additional HCl dipping [1] does not change anything on copper signals.

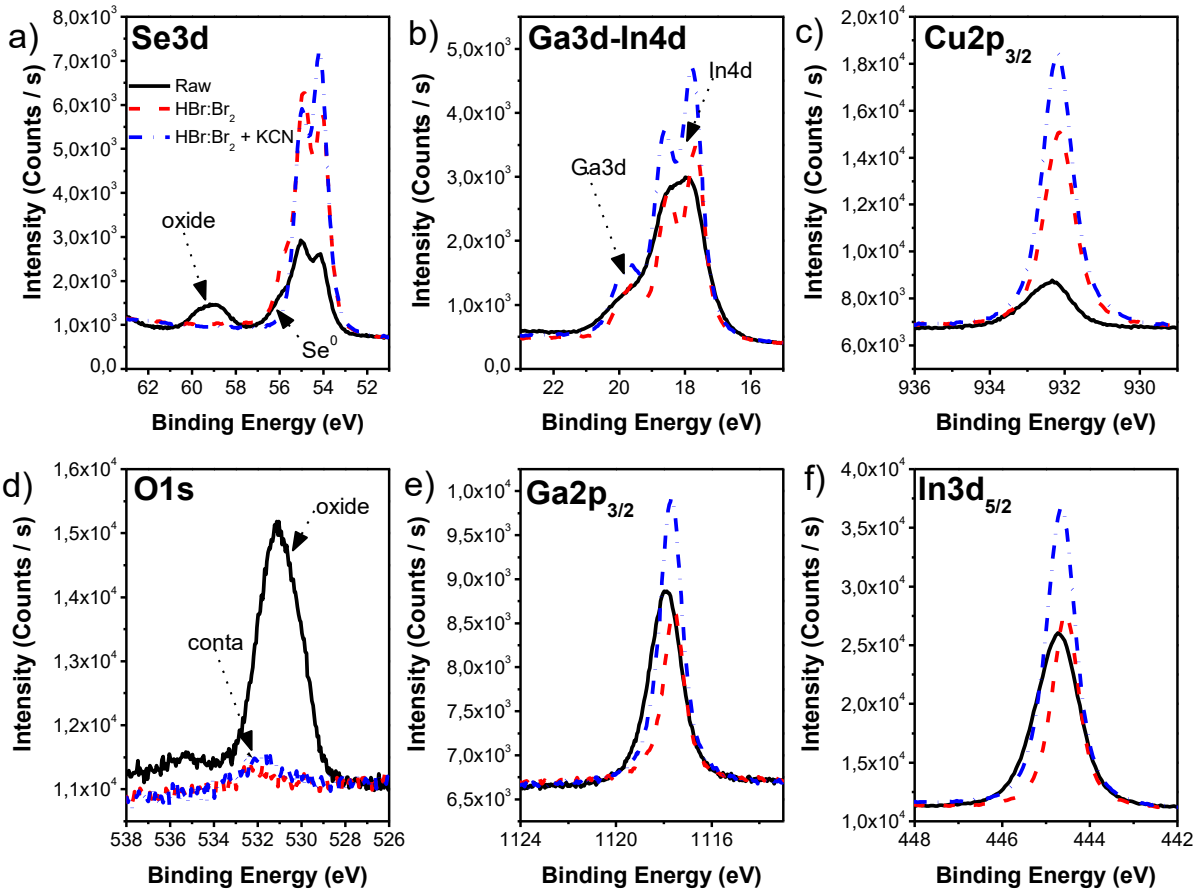

Figure 1: High energy resolution XPS spectra comparison of as-grown (solid black line)// etched with $HBr:Br_2$ H_2O solution (dash red line) // etched with $HBr:Br_2:H_2O$ solution and KCN treated (dash-dot blue line) CIGS surface: a) Se3d, b) Ga3d-In4d region, c) $Cu2p_{3/2}$, d) O1s, e) $Ga2p_{3/2}$ and f)$In3d_{5/2}$.

The analysis of $Cu2p_{3/2}$, $In3d_{5/2}$, $Ga2p_{3/2}$, Se3d and O1s photopeaks shows that after the final KCN treatment a very clean surface without selenide phase and detectable oxides is obtained. The oxygen signal intensity is very low and only related to adventitious carbon stacked to the surface during the sample manipulations. This suggests that $Ga2p_{3/2}$, $In3d_{5/2}$, $Cu2p_{3/2}$ and Se3d energy distributions substantially narrowed, are representative of only one chemical environment: the CIGS one's. This diagnostic will be refined later in the text but this first examination of the photopeaks evolution demonstrates that a clean CIGS surface is obtained at the issue of the combined sequences. At first sight, the surface differs from a perfect reference only due to carbon sticking at the surface during the transfer. The adventitious carbon contamination is very difficult to evaluate due to $SeL_3M_{23}M_{45}$/C1s overlapping (Figure 2) and will not be quantified here.

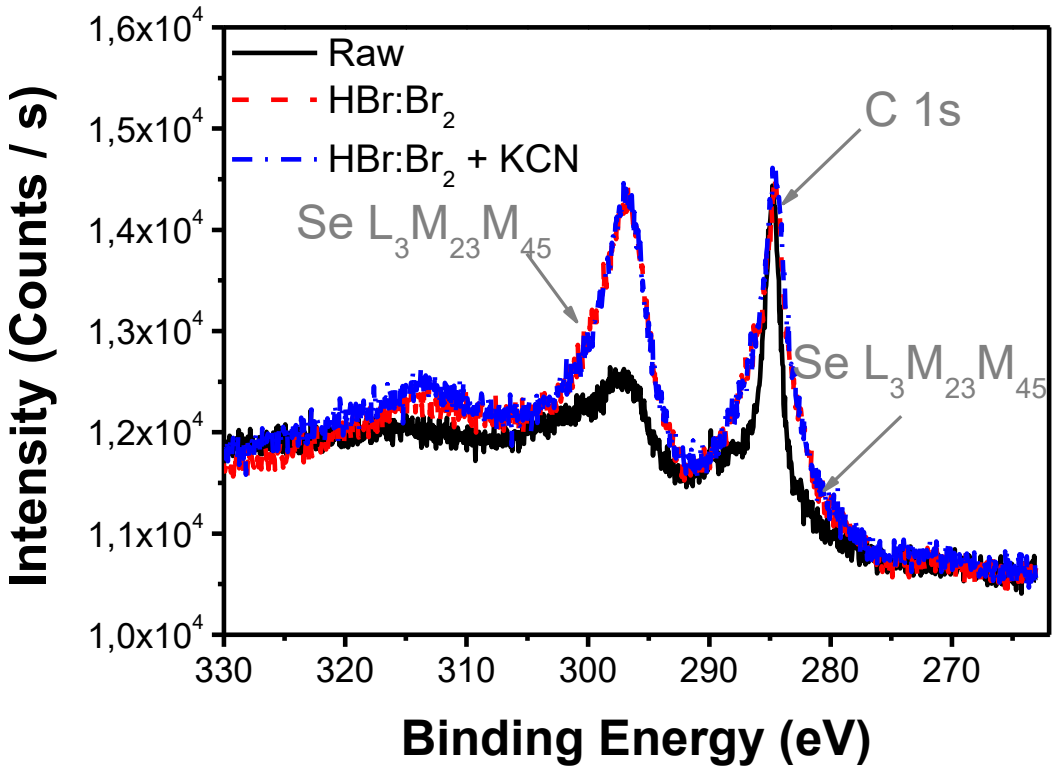

Figure 2: C1s XPS spectra comparison as-grown (solid black line)// etched with HBr:Br2 H2O solution (dash red line) // etched with HBr:Br2:H2O solution and KCN treated (dash-dot blue line) CIGS surface.

Corrected XPS peaks intensities provide the XPS global chemical composition using the corresponding sensitivity factors (SF($Cu2p_{3/2}$): 18.147, SF($Ga2p_{3/2}$): 22.700, SF($In3d_{5/2}$): 19.112, SF(Se3d): 1.600 and SF (O1s): 2.881), the respective electron attenuation lengths and the transmission function of the analyzer. The resulting atomic percentages are presented in Table 1.

Table 1: Atomic percentages of CIGS surfaces obtained from the $Cu2p_{3/2}$, $Ga2p_{3/2}$, $In3d_{5/2}$, Se3d and O1s regions for different surface treatments; C1s contribution is not considered

Atomic percentage (%)	Cu	Ga	In	Se	O
Raw surface	4.0	5.1	13.5	33.5	43.9
HBr:Br_2 surface	12.6	3.7	11.1	69.0	3.6
HBr:Br_2 + KCN surface	15.1	5.4	15.9	58.2	5.4

The direct calculation of the surface composition presented in Table 1 assumes that the layer is homogeneous within the matter probed by XPS. This is verified by XPS mapping. Moreover, the signal correction steps are complex, then the deduced XPS compositions must be used with a critical reasoning about a possible difference between the actual chemical composition and the XPS extracted one. Note that if we consider the C1s contribution, its intensity can be roughly estimated without a complete fitting procedure and give atomic percentage contribution for the carbon between 30-50% in a global composition, the corrected contribution for the other elements remaining in the same relative proportions.

With our nearly “perfect-CIGS surface”, the GGI, obtained thanks to the Ga2p and In3d regions ($GGI_{Ga2pIn3d}$), reaches the value of 0.25 (± 0.01) (0.27 and 0.25 for raw and HBr:Br_2 surfaces , respectively) when the expected value is 0.30. This probable under-estimation can be explained by the adventitious carbon over-layer acting, previously mentioned, as differential attenuation layer

depending on the KE of the photoelectrons. Concerning CIGS it is a key point because the foremost usual lines used are $Ga2p_{3/2}$ (KE: 370.6 eV), $Cu2p_{3/2}$ (KE: 555.6 eV), $In3d_{5/2}$ (KE: 1043.6 eV) and Se3d (KE: 1429.6 eV) whose photopeak kinetic energies are largely distributed over the 1486.6 eV range provided by the X-Ray Al anode. Then, corrections due to the carbon overlayer attenuation must be considered. Obviously, the differential attenuation is as a perturbation source for the apparent XPS composition and very difficult to deal with due to the fluctuation on the nature of the adventitious carbon contamination and complicated by its possible inhomogeneous sticking at the surface. As indicated above, the determination of the C content is not obvious requires to separate the C1s from Se($L_3M_{23}M_{45}$) lines (Figure 2) and, so, rarely considered. In addition, specific calibration to determine the differential attenuations is required. Another possibility consists in minimizing this effect by choosing a set of XPS peak with narrower distribution of KE, as previously proposed by Bär et al. [16,17].

CIGS's XPS response provides this opportunity through its Ga3d and In4d levels (Figure 1-b), appearing in the 30 eV to 10 eV spectral region. Then, we can work without differential signal balancing consideration. Moreover equal escape depths can be assumed for this set of lines and an absolute estimation of the GGI response of the material. Then, the only questionable parameters are the sensitivity factors ones. As the element III's distribution is grouped only over 6 eV range, the separation is sufficient between both to provide coherent fitting procedure when the CIGS surface is oxide free.

To ensure a reliable modeling procedure, so a fine determination of the reconstruction parameters is necessary, we choose to perform the Ga3d-In4d region reconstruction of a certified and deoxidized $In_xGa_{1-x}As/InP$ epilayer reference sample ($In_{0.517}Ga_{0.483}As$) Note that as expected, the relative energy position and intensities are totally reproducible on XPS mapping The comparison of the Ga3d-In4d region of the reference $In_xGa_{1-x}As/InP$ and CIGS layers is presented Figure 3-a. Both global shapes are similar, the main difference relying on the Ga and In contents in the two materials. The fitting

parameters have been compared to the one obtained on GaP and InP samples (same experimental conditions) for which only one fingerprint, either Ga or In, is visible.

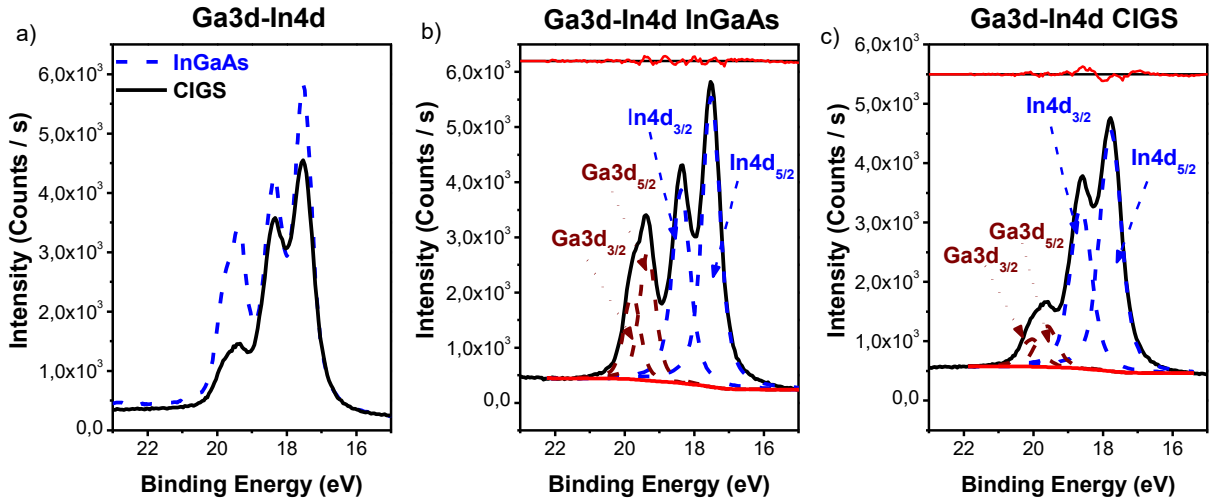

Figure 3: High energy resolution XPS spectra comparison of CIGS (black solid line) and $In_xGa_{1-x}As$ (blue dash line) materials -a)- and simulations of b) $In_xGa_{1-x}As$ and c) CIGS Ga3d-In4d regions.

Figure 3-b and Figure 3-c present the fitting simulations obtained for the Ga3d-In4d region for the $In_xGa_{1-x}As$ and CIGS layers. For both, the main constraints introduced in the simulation are related to the branching ratio (close to 0.67 $\pm$ 0.01), as Ga3d and In4d present a d-level spin-orbit splitting, and to the FWHM (Full Width at Half Maximum) values, which are considered as equal for the 3/2 and 5/2 d contributions. Concerning In4d, the spin-orbit splitting is perfectly established and obviously the same for both layers, as soon as a correct deoxidation has been performed. Its value is equal to 0.85 $\pm$ 0.01 eV. Regarding the spin-orbit splitting for Ga3d, it is less marked and needs very high resolution spectra to observe characteristic shape deformation. For the $In_xGa_{1-x}As$ layer, the spin-orbit splitting seems more resolved. So, using this support, the spin-orbit distance found for the Ga3d level is equal to 0.44 $\pm$ 0.02 eV, in total agreement with our oxide free GaP samples (0.43 $\pm$ 0.02 eV). Using these fitting parameters, we obtain good simulation of the key Ga3d-In4d regions which has characteristic intensity ratios related to the atomic ratio between Ga and In present in $In_xGa_{1-x}As$ or CIGS layers. When the respective intensities are corrected from the atomic level sensitivity factors,

we access to the XPS $GGI_{Ga3dIn4d}$ parameter. For our $In_xGa_{1-x}As$ sample, a GGI equal to 0.484 $\pm$ 0.005 is determined using a factor sensitivity ratio (SF) SF_{Ga3d}/SF_{In4d} (1.412/3.601) equal to 0.39 (THERMO@ Avantage Scientific data base). The XPS GGI deduced from the Ga3d-In4d region is then in perfect agreement with the GGI (0.483) obtained by XRD, thereby validating the fitting parameters used.

The fitting parameters (branching ratio, spin-orbit splitting) obtained thanks to the reference sample were then implemented to the Ga3d-In4d region of the CIGS sample (Figure 3-c) using the same previous procedure. The $GGI_{Ga3dIn4d}$ ratio is equal to 0.29 (± 0.01), which presents much more coherence than the $GGI_{Ga2pIn3d}$ ratio (0.25 ± 0.01) presented above. In addition, an interesting difference is observed between the $In_xGa_{1-x}As$ reference sample and the CIGS ones. Indeed, a widening of the FWHM parameters for each element is noted to satisfactorily fit the CIGS Ga3d-In4d region (Table 2). As information, FWHM for GaP and InP materials are also presented in Table 2, which are equal to ones determine for $InxGa_{1-x}As$ sample.

Table 2: FWHM parameters evolution for GaP, InP, $In_xGa_{1-x}As$ and CIGS layers

FWHM parameter (eV)	$In4d_{5/2}$	$In4d_{3/2}$	$Ga3d_{5/2}$	$Ga3d_{3/2}$
GaP	/	/	0.55	0.55
InP	0.63	0.63	/	/
$In_xGa_{1-x}As$	0.62	0.62	0.55	0.55
CIGS	0.74	0.74	0.71	0.71

To explain this widening on FWHM CIGS layer, several possibilities must be considered. As CIGS is a polycrystalline material, a surface potential modulation could be considered, associated to the grain boundaries distribution. Therefore, a slight modulation of the energy diagram can appear leading to

250 the widening of the FWMH photopeaks. Working with a CIGS monocrystal will remove this effect and
251 provide a more accurate support for discussion.

252 4. Conclusion

253 With a combination of chemical treatments (acidic Br_2 etching followed by KCN dipping), a CIGS
254 "reference" surface was obtained as support for GGI quantification obtained by XPS. From this
255 reference surface, clean of residual oxides and side selenide phases, a determination of the GGI ratio,
256 is then optimized. Comparing the $GGI_{Ga3dIn4d}$ (0.29 ± 0.01) and the $GGI_{Ga2p,\ In3d}$ (0.25 ± 0.01), we
257 observe a slight but consequent difference. We attribute it to possible perturbations induced by the
258 signals attenuation due to carbon contamination. Considering that the Ga3d-In4d region is restricted
259 in an energy window of 10 eV, we assume that the attenuation effect is limited even nonexistent,
260 suggesting that this window would be the most adapted to the quantification of GGI [16,17].
261 However, this hypothesis needs correcting factors provided by library data bases to be accurate
262 accurate, and particularly the sensitivity factors which, in this case, can be considered as the only one
263 significant correction parameters. In order to comfort the validity of the sensitivity factors employed
264 for the Ga3d-In4d region, we introduced, as reference sample, an III-V epitaxial layer $In_xGa_{1-x}As$
265 whose composition has been certified by XRD measurements. This epitaxial layer presents a similar
266 Ga3d-In4d mixed window. On this reference sample, we determine the fitting parameters and we
267 deduce a final XPS composition in total agreement with the expected one, validated by XRD
268 measurements. So we consider that our correcting factors are validated. Therefore we apply these
269 fitting parameters to the determination of the $GGI_{Ga3dIn4d}$ on CIGS, which can now be considered as
270 the actual GGI value at the surface. Moreover, we observe a slight widening of the XPS lines,
271 interrogating on the small fluctuations of the potential at the surface. Finally, the lower GGI value
272 obtained using regular core levels (Ga2p and In3d) can be consider as under-estimated, indicating
273 that the perturbation of Ga2p intensity is more affected than the In3d's one. This observation is
274 coherent with the evolution of kinetic energies, as the Ga2p one is lowest than the In3d's one,

leading to a Ga2p peak more affected by the attenuation layer than In3d's one. According to the carbon contamination level, the $GGI_{Ga2p,\ In3d}$ determination can be underestimated, whereas the $GGI_{Ga3dIn4d}$ won't be affected. To reduce the carbon contamination, different chemical engineering treatments should be provided. Similarly, ionic Argon cluster bombardment can also be used. Both points will be extensively presented in a following paper. Furthermore, other key parameters such as CGI and Se balance can be studied using combinations in similar energy ranges [20].

5. Acknowledgements

Authors thank Wolfram Hempel from ZSW (Zentrum für Sonnenenergie- und Wasserstoff-Forschung, Germany) for CIGS samples supply.

Authors thank François Jomard (GEMAC, UVSQ) for SIMS measurements.

This work has been carried out in the framework of the project I of IPVF (Institut Photovoltaïque d'Ile-de-France). This project has been supported by the French Government in the frame of the program "Programme d'Investissement d'Avenir – ANR-IEED-002-01".

6. References

[1] A. Loubat, M. Bouttemy, S. Gaiaschi, D. Aureau, M. Frégnaux, D. Mercier, J. Vigneron, P. Chapon, A. Etcheberry, Chemical engineering of Cu(In,Ga)Se_2 surfaces: An absolute deoxidation studied by X-ray Photoelectron Spectroscopy (XPS) and Auger Electron Spectroscopy (X-AES) signatures, Thin Solid Films. 633 (2016) 87-91.

[2] K. Orgassa, U. Rau, H.W. Schock, I.U. Werner, Optical constants of Cu (ln, Ga) Se_2 thin films from normal incidence transmittance and reflectance, in: Photovoltaic Energy Conversion, 2003. Proceedings of 3rd World Conference On, IEEE, 2003: pp. 372–375.

[3] S. Minoura, K. Kodera, T. Maekawa, K. Miyazki, S. Niki, H. Fujiwara, Dielectric function of Cu(In,Ga)Se_2-based polycrystalline materials, Journal of Applied Physics. 113 (2013) 063505.

[4] S. Minoura, T. Maekawa, K. Kodera, A. Nakane, S. Niki, H. Fujiwara, Optical constants of Cu(In, Ga)Se_2 for arbitrary Cu and Ga compositions, Journal of Applied Physics. 117 (2015) 195703.

[5] S. Levcenko, L. Durán, G. Gurieva, M.I. Alonso, E. Arushanov, C.A. Durante Rincón, M. León, Optical constants of $Cu(In_{1-x}Ga_x)_5Se_8$ crystals, Journal of Applied Physics. 107 (2010) 033502-033506.

[6] S. Levcenko, G. Gurieva, E.J. Friendrich, J. Trigo, J. Ramiro, J.M. Merino, E. Arushanov, M. Leon, Optical constants of $CuIn_{1-x}Ga_xSe_2$ films deposited by flash evaporation, Mold. J. Phys. Sciences. 9 (2010) 148–155.

[7] M.I. Alonso, M. Garriga, C.A. Durante Rincón, E. Hernández, M. León, Optical functions of chalcopyrite $CuGa_xIn_{1-x}Se_2$ alloys, Applied Physics A: Materials Science & Processing. 74 (2002) 659–664.

[8] P.D. Paulson, R.W. Birkmire, W.N. Shafarman, Optical characterization of $CuIn_{1-x}Ga_xSe_2$ alloy thin films by spectroscopic ellipsometry, Journal of Applied Physics. 94 (2003) 879.

[9] M. Richter, C. Schubbert, P. Eraerds, I. Riedel, J. Keller, J. Parisi, T. Dalibor, A. Avellán-Hampe, Optical characterization and modeling of $Cu(In,Ga)(Se,S)_2$ solar cells with spectroscopic ellipsometry and coherent numerical simulation, Thin Solid Films. 535 (2013) 331–335.

[10] B. Canava, J. Vigneron, A. Etcheberry, D. Guimard, J.-F. Guillemoles, D. Lincot, S.O.S. Hamatly, Z. Djebbour, D. Mencaraglia, XPS and electrical studies of buried interfaces in Cu(In, Ga)Se_2 solar cells, Thin Solid Films. 403 (2002) 425–431.

[11] K. Ramanathan, F.S. Hasoon, S. Smith, D.L. Young, M.A. Contreras, P.K. Johnson, A.O. Pudov, J.R. Sites, Surface treatment of $CuInGaSe_2$ thin films and its effect on the photovoltaic properties of solar cells, Journal of Physics and Chemistry of Solids. 64 (2003) 1495–1498.

[12] J. Lehmann, S. Lehmann, I. Lauermann, T. Rissom, C.A. Kaufmann, M.C. Lux-Steiner, M. Bär, S. Sadewasser, Reliable wet-chemical cleaning of natively oxidized high-efficiency Cu(In,Ga)Se_2 thin-film solar cell absorbers, Journal of Applied Physics. 116 (2014) 233502.

[13] B. Canava, J. Vigneron, A. Etcheberry, J.F. Guillemoles, D. Lincot, High resolution XPS studies of Se chemistry of a Cu(In,Ga)Se_2 surface, Applied Surface Science. 202 (2002) 8–14.

[14] O. Roussel, M. Lamirand, N. Naghavi, J.F. Guillemoles, B. Canava, A. Etcheberry, Interfacial chemistry control in thin film solar cells based on electrodeposited $CuIn(S,Se)_2$, Thin Solid Films. 515 (2007) 6123–6126.

[15] M. Bouttemy, P. Tran-Van, I. Gerard, T. Hildebrandt, A. Causier, J.L. Pelouard, G. Dagher, Z. Jehl, N. Naghavi, G. Voorwinden, B. Dimmler, M. Powalla, J.F. Guillemoles, D. Lincot, A. Etcheberry, Thinning of CIGS solar cells: Part I: Chemical processing in acidic bromine solutions, Thin Solid Films. 519 (2011) 7207–7211.

[16] M. Bär, I. Repins, M. A. Contreras, L. Weinhardt, R. Noufi C. Heske, Chemical and electronic surface structure of 20%-efficient Cu(In,Ga)Se_2 thin film solar cell absorbers, Applied Physics Letters. 95 (2009) 052106-052109.

[17] E. Handick, P. Reinhard, R. G. Wilks, F. Pianezzi, T. Kunze, D.r Kreikemeyer-Lorenzo, L. Weinhardt, M. Blum, W. Yang, M. Gorgoi, E. Ikenaga, D. Gerlach, S. Ueda, Y. Yamashita, T. Chikyow, C. Heske, S. Buecheler, A. N. Tiwari, M. Bär, Formation of a K-In-Se Surface Species by NaF/KF Postdeposition Treatment of Cu(In,Ga)Se_2 Thin-Film Solar Cell Absorbers, Applied Materials & Interfaces. 9 (2017) 3581-3589.

[18] B. Dimmler, H.W. Schock, Scaling-up of CIS Technology for Thin-film Solar Modules, Progress in Photovoltaics: Research and Applications. 4 (1996) 425–433.

[19] A. Loubat, C. Eypert, F. Mollica, M. Bouttemy, N. Naghavi, D. Lincot, A. Etcheberry, Optical properties of ultrathin CIGS films studied by spectroscopic ellipsometry assisted by chemical engineering, Applied Surface Science. 421 (2017) 643–650.

[20] M. Bär, J. Klaer, R. Félix, N. Barreau, L. Weinhardt, R. G. Wilks, Cl. Heske, H.-W. Schock, Surface Off-Stoichiometry of $CuInS_2$ Thin-Film Solar Cell Absorbers, IEEE Journal of Photovoltaics, 3, (2013), 828-832.

List of Figures and Captions

Figure 1: High energy resolution XPS spectra comparison of as-grown (solid black line)// etched with HBr:Br_2 H_2O solution (dash red line) // etched with HBr:Br_2:H_2O solution and KCN treated (dash-dot blue line) CIGS surface: a) Se3d, b) Ga3d-In4d region, c) $Cu2p_{3/2}$, d) O1s, e) $Ga2p_{3/2}$ and f)$In3d_{5/2}$.

Figure 2: C1s XPS spectra comparison as-grown (solid black line)// etched with HBr:Br_2 H_2O solution (dash red line) // etched with HBr:Br_2:H_2O solution and KCN treated (dash-dot blue line) CIGS surface.

Figure 3: High energy resolution XPS spectra comparison of CIGS (black) and InGaAs (blue) materials - a)- and simulations of b) InGaAs and c) CIGS Ga3d-In4d regions.

Table 1: Atomic percentages of CIGS surfaces obtained from the $Cu2p_{3/2}$, $Ga2p_{3/2}$, $In3d_{5/2}$, Se3d and O1s regions for different surface treatments; C1s contribution is not considered

Table 2: FWHM parameters evolution for GaP, InP, $In_xGa_{1-x}As$ and CIGS layers